

Kilohertz QPO Frequency and Flux Decrease in AQL X-1 and Effect of Soft X-ray Spectral Components

W. Yu¹, T. P. Li¹, W. Zhang², S. N. Zhang^{3,4}

ABSTRACT

We report on an RXTE/PCA observation of Aql X-1 during its outburst in March 1997 in which, immediately following a Type-I burst, the broad-band 2-10 keV flux decreased by about 10% and the kilohertz QPO frequency decreased from 813 ± 3 Hz to 776 ± 4 Hz. This change in kHz QPO frequency is much larger than expected from a simple extrapolation of a frequency-flux correlation established using data before the burst. Meanwhile a very low frequency noise (VLFN) component in the broad-band FFT power spectra with a fractional root-mean-square (rms) amplitude of 1.2% before the burst ceased to exist after the burst. All these changes were accompanied by a change in the energy spectral shape. If we characterize the energy spectra with a model composed of two blackbody (BB) components and a power law component, almost all the decrease in flux was in the two BB components. We attribute the two BB components to the contributions from a region very near the neutron star or even the neutron star itself and from the accretion disk, respectively.

Subject headings: X-ray: stars - stars: individual (Aquila X-1) - stars: neutron

1. Introduction

Kilohertz QPOs have been observed in about 20 low-mass X-ray binaries by the *Rossi X-ray Timing Explorer* (RXTE) since its launch at the end of 1995 (van der Klis 1998). Although the detail production mechanism of these QPOs is not fully understood, there is little doubt that they correspond to the dynamical time scale near the neutron star surface, and as such they enable us to probe strong gravity effects and the equation of state of neutron stars (Kaaret et al. 1997; Zhang, W. et al. 1996; van der Klis 1998; Miller et al. 1997; Lamb et al. 1998).

The kHz QPO frequency has been found to correlate with at least two quantities: source count rate or flux and energy spectral shape or hardness ratios (van der Klis 1998 and references

¹LCRHEA, Institute of High Energy Physics, Beijing 100039, China

² Laboratory for High Energy Astrophysics, Goddard Space Flight Center, Greenbelt, MD 20771

³ University of Alabama in Huntsville, Department of Physics, Huntsville, AL 35899

⁴ NASA/Marshall Space Flight Center, ES-84, Huntsville, AL 35812

therein; Kaaret et al. 1998; Zhang, W. et al. 1998b; Mendéz et al. 1999). Soft X-ray transients like 4U 1608-52 and Aql X-1, with their large swings in both count rates and energy spectral shapes, are ideal for the study of these kinds of correlations. 4U 1608-52 and Aql X-1 have both been observed with RXTE/PCA during their outburst decay. A similar correlation between the QPO frequency and the X-ray flux has been observed in different flux ranges (Yu et al. 1997; Mendéz et al. 1998; Zhang, W. et al. 1998a). In each flux range, the QPO frequency appears correlated with the X-ray flux. Spectral studies suggest that there is a significant correlation between the QPO frequency and the spectral shape even among data from different flux ranges in 4U 1608-52 (Kaaret et al. 1998). A correlation between the QPO frequency and the spectral shape has also been found in other QPO sources. For example, a correlation between the QPO frequency and the flux of the blackbody component was observed in 4U 0614+091 (Ford et al. 1997).

The QPO frequency is usually regarded as the Keplerian frequency at the inner disk radius or its beat frequency with the neutron star spin in the beat-frequency model (Alpar and Shaham 1985; Lamb, et al. 1985; Strohmayer et al. 1996; Zhang, S. N. et al. 1998; Miller et al. 1996). The higher the mass accretion rate, the higher should be the QPO frequency. This will lead to a correlation between the QPO frequency and the flux. However, when a transition of the accretion state happens, same mass accretion rate may correspond to different inner disk radii and different fluxes before and after the transition. A spectral variation is probably associated with a variation of the accretion state, and might lead to a new flux range or frequency range. Comparison of the spectral components before and after the spectral variation and study of the correlation between QPO frequency and the spectral shape will help to reveal how the kHz QPOs are generated.

In this letter, we present our study with the RXTE/PCA data before and after an X-ray burst in Aql X-1.

2. Observations and Data Analysis

An X-ray burst with a peak PCA count rate above 40,000 cps was observed by RXTE/PCA on March 1, 1997, when the daily-averaged ASM count rate is ~ 4 cps. Nearly coherent oscillation at about 549 Hz was detected in the X-ray burst. A $\sim 10\%$ flux decrease and a corresponding QPO frequency decrease were observed after the X-ray burst (Zhang, W. et al. 1998a). The count rate decrease is ~ 64 cps in the entire PCA band. The data used for timing analysis in the kHz frequency range is taken in the event mode *E_125us_64M_0_1s*. The energy range 2-10 keV was selected, the same as those used in Zhang et al. (1998a). The *Standard 1* data is used to study the frequency range below 0.5 Hz. The *Standard 2* data is used in the spectral analysis. All the errors quoted in the following are 1σ errors. The low energy response of the RXTE/PCA detectors is not sufficient in constraining the absorption column density N_H . We have fixed it at 3.0×10^{21} cm $^{-2}$ in our spectral fittings, according to previous studies (Czerny et al. 1987; Verbunt, et al. 1994; Zhang, S. N. et al. 1998).

2.1. Timing Analysis

We first calculate the dynamical power spectra around the X-ray burst. Then a model composed of a constant and a Lorentzian function is fit to the 200-2000 Hz power spectra to determine the QPO frequency. In Fig. 1, we show the light curve around the X-ray burst and how QPO frequency evolved. The QPO frequency decreased from about 813 ± 3 Hz before the burst to 776 ± 4 Hz after the burst. In Fig. 2, the QPO frequency vs. PCA count rate (CR) in the energy range 2-10 keV is shown for the observation of two consecutive RXTE orbits on March 1. The data points on the lower-left corner are taken after the X-ray burst, and those points on the right side branch are taken before the X-ray burst. We apply a linear model to fit the right side branch and get $f_{qpo} = -(219.4 \pm 32.0) + (1.954 \pm 0.002) \times CR$. The average count rate after the X-ray burst in 2-10 keV band is ~ 478 cps, the inferred QPO frequency from the above QPO frequency vs. count rate relation at this count rate is 714 ± 30 Hz. Thus the inferred QPO frequency decrease is about 99 ± 30 Hz, more than twice of the observed frequency decrease of 37 ± 5 Hz.

In order to study the source variability at frequencies lower than 0.5 Hz, we divide the light curve into 256 s segments, then calculate the power spectrum of each segment. We average 16 power spectra before the X-ray burst and 4 power spectra after the burst. In Fig. 3, we show the average Leahy normalized power spectra in the frequency range 0.002-0.5 Hz before and after the X-ray burst. The power spectrum before the X-ray burst shows a very low frequency noise (VLFN) component of a power law form (Hasinger & van der Klis 1989). A model composed of a white noise level of 2 and a power law component is fit to the average power spectra. We obtain a power law index $\alpha = 1.5 \pm 0.2$ and $A = 0.0024 \pm 0.0015$. The fractional root-mean-square (*rms*) variability of the VLFN is about $1.2 \pm 0.4\%$. The power spectrum after the X-ray burst is consistent with a white noise.

2.2. Spectral Analysis

The energy spectrum of Aql X-1 has changed little during the outburst before March 1 (Zhang, W. et al. 1998a) and was of a blackbody type. In subsequent observations, the energy spectra gradually changed from a blackbody type to a blackbody plus a power-law type (see Zhang, S. N. et al. 1998). The spectra before and after the X-ray burst are shown in Fig. 4. In Fig. 4(a), we plot the ratio between the spectra (2-10 keV) before and after the X-ray burst, namely spectrum $N_1(E)$ and spectrum $N_2(E)$, respectively. The ratio as a function of energy is not a constant. The flux decrease is more severe above 5 keV. Thus a variation of the spectral shape was associated with the flux decrease.

Spectral models of a single blackbody (BB), a single power law (PL) and their combination (BB+PL) can not yield an acceptable fit to both spectra $N_1(E)$ and $N_2(E)$ in the energy range 3-20 keV. The model composed of two BB components and a PL component gives an acceptable fit. The inclusion of two BB components, one of which may be a multi-color disk (MCD) component,

has been applied previously to the soft X-ray transient 4U 1608-52 during an outburst (Mitsuda et al. 1984) and Aql X-1 during an outburst rise (Cui et al. 1998). In Table 1, we list the parameters of the spectral fit to both spectra with 2BB+PL and BB+MCD+PL models. The emission area of the ~ 0.26 keV BB component in the 2BB+PL model fit is much larger than the surface area of a neutron star. This suggests that it may be a disk component and the fit with BB+MCD+PL model may be reasonable. Assuming the disk inclination angle as zero, we find that the apparent inner disk radius is in the 1σ range 200-470 km. In both spectra, the PL components only contribute less than 1/20 of the total flux in the energy range 2-10 keV. The difference between the average PCA count rate (> 10 keV) before and after the X-ray burst is 0.64 ± 0.38 cps. This indicates that the PCA flux variation mainly comes from the spectral components in the soft X-ray range below 10 keV.

The two BB temperatures are stable during the flux decrease as shown in Table 1. Thus it is reasonable to study the flux decrease by subtracting the spectrum $N_2(E)$ from the spectrum $N_1(E)$. In Fig. 4(b), we plot the subtracted spectrum ($N_1(E) - N_2(E)$) in the energy range 2-10 keV. A model composed of two BB components yields an acceptable fit to this spectrum, which is also plotted. In Table 2, we list the best-fit parameters and the fluxes of the two components. The 2-10 keV energy flux of the residual spectrum is about $(7 \pm 2)\%$ of that of the total before the X-ray burst. The subtraction of the PL components in Table 1 mainly affects the 0.28 keV component shown in Fig. 4(b), i.e. a flux of 0.7 ± 2.5 photons $\text{cm}^{-2} \text{ s}^{-1}$ in 2-4 keV.

3. Discussion and Conclusion

We have reported that there was a simultaneous decrease of the X-ray flux, the QPO frequency, and the VLFN component in Aql X-1 immediately following a Type-I X-ray burst. The decrease lasted at least 400 s until the observation was stopped. The flux decrease was mainly due to a decrease of the spectral components in the energy range below 10 keV. As a type I X-ray burst only occurs when the condition for the thermonuclear instability is met, the X-ray burst and the flux decrease may be causally related.

The X-ray flux derived from the spectral fit in Table 1 has an uncertainty as large as 20%, which is insufficient to determine the decrease of the X-ray luminosity. However, the spectral fit shown in Table 2 yields more confined parameters, suggesting that there is a $(7 \pm 2)\%$ decrease of the X-ray luminosity in 2-10 keV. The index of the PL component decreases together with the decrease of the X-ray luminosity. This behavior is similar to that found in 4U 1608-52 and 4U 0614+091 (Kaaret et al. 1998).

The spectral parameters of the two BB components in Table 1 seems consistent with the trend shown in Fig.2 of Cui et al. 1998, i.e. the lower the ASM count rate of Aql X-1, the larger the inner disk radius and the lower the BB temperatures are. The ~ 1.06 keV BB is probably related to a part of the neutron star surface. The decrease of the VLFN after the burst supports

the idea. The VLFN in LMXBs is an indication of the time-dependent fusion reactions (fires) on the neutron star surface (Bildsten 1993), which corresponds to a mass accretion rate larger than that of the bursting stage. The disappearance of the VLFN in Aql X-1 then not only suggests that at least a few percent of the observed X-ray flux was from the fusion reaction on the neutron star surface before the X-ray burst, but also indicates that after the X-ray burst, the time-dependent fusion reactions were probably stopped. This may indicate that the X-ray burst had consumed almost all the nuclear fuel on the neutron star, and the stop of the time-dependent fusion reaction contributes to a significant part of the 7% X-ray flux decrease.

The inner disk radii before and after the X-ray burst, derived from Table 1, are about 300 km and 360 km, respectively. For an accreting neutron star of $2.0 M_{\odot}$ and taking $\cos(\theta)=1$, the upper limits on the Keplerian frequencies corresponding to the two radii are 15 and 12 Hz. The spectral hardening would lead to an even larger inner disk radius thus an even lower frequency (Shimura & Takahara 1995). On the other hand, the QPO frequency around 800 Hz is probably the lower of the twin peaks, which suggests that the Keplerian frequency at the inner edge of the disk should be around 1075 Hz (Zhang, W. et al. 1998a). Thus the derived inner disk radii are inconsistent with the beat-frequency model. The difference between the observed QPO frequency and those inferred from the spectral fit probably comes from a lack of detailed knowledge of the spectral components in neutron star X-ray binaries, and the lack of sensitivity below 2 keV of the PCA to determine the parameters of a 0.26 keV blackbody spectral component. Conversely, it is also possible that the identification of the kHz QPOs as the Keplerian frequency at the inner edge of the accretion disk or its beat frequency against the neutron star spin is incorrect.

The observed QPO frequency decrease is 37 ± 5 Hz, about 1/3 of that inferred from the QPO frequency vs. count rate relation. In principle, the decrease of the disk BB flux should originate from a decrease of the mass accretion rate. This would introduce a decrease of the QPO frequency. Taking the spectral parameters in Table 2 and using the PCA instrumental information, we estimate that the 2-10 keV PCA count rate of the disk BB is 23 ± 8 cps, and that of the neutron star BB component is 47 ± 6 cps. So the QPO frequency decrease is consistent with the 23 cps count rate decrease of the disk BB component, which is about 1/3 of the total decrease of ~ 70 cps. Because the PCA effective area is not a constant with photon energy, and the two BB components have quite different BB temperatures, the incident BB photon fluxes (Table 2) can not replace the above count rate estimates when we study the frequency decrease inferred from the PCA count rate.

The central radiation force may also affect the QPO frequency. A decrease of the central BB emission from near the neutron star surface would probably introduce an increase of the QPO frequency. Thus two mechanisms would account for the correlation between the QPO frequency and the count rate in Fig. 2. One is that it is the disk BB flux instead of the total flux that is correlated with the QPO frequency. The QPO frequency variations between the data points on the right side branch in Fig. 2 originate from the disk BB flux variations. Thus the data points on the lower left corner may join in the data points of the right side branch in a plot of the QPO

frequency vs. the disk BB flux. The other is that a decrease of the central BB radiation force after the X-ray burst would increase the QPO frequency, then the QPO frequency did not follow the correlation relation when the central BB radiation force is nearly constant. Our study indicates that a comprehensive investigation on the correlation between QPO frequency and each spectral component is needed, especially when a flux decrease or spectral transition occurs.

We thank an anonymous referee for helpful comments and suggestions, which certainly improved this article. This work was supported by the National Natural Science Foundation of China under grant 19673010 and 19733003.

REFERENCES

Alpar, A. and Shaham, J. 1985, *Nature*, 316, 239

Bildsten, L. 1993, *ApJ*, 418, L21

Cui, W. et al. 1998, *ApJ*, 502, L49

Czerny, M., Czerny, B. & Grindlay, J. E. 1987, *ApJ*, 312, 122

Ford, E. et al. 1997, *ApJ*, 486, L47

Hasinger, G., van der Klis, M. 1989, *A&A*, 225, 79

Kaaret, P., Ford, E.C., and Chen, K. 1997, *ApJ*, 480, L27

Kaaret, P., Yu, W., Ford, E. C., Zhang, S. N. 1998, 497, L93

Lamb, F. K., Shibasaki, N., Alpar, M. A. and Shaham, J. 1985, *Nature*, 317, 681

Lamb, F. K., Miller, M. C., and Psaltis, D. 1998 (astro-ph/9802348)

Mendéz, M. et al. 1998, *ApJ*, 494, L65

Mendéz, M. et al. 1999, *ApJ*, 511, L49 (astro-ph/9811261)

Miller, M.C., Lamb, F.K., and Psaltis, D. 1998, submitted to *ApJ* (astro-ph/9609157)

Miller, M.C., and Lamb, F.K. 1998, *ApJ*, 499, L37 (astro-ph/9711325)

Mitsuda, K. et al. 1984, *PASJ*, 36, 741

Shimura, T. and Takahara, F. 1995, *ApJ*, 445, 780

Strohmayer, T. et al. 1996, *ApJ*, 469, L9

van der Klis, M. 1998, to appear in the Proceedings of the Third William Fairbank Meeting
(astro-ph/9812395)

Verbunt, E., et al. 1994, A&A, 285, 903

Yu, W. et al. 1997, ApJ, 490, L153

Zhang, S.N., Yu, W. and Zhang, W. 1998, ApJ, 494, L71

Zhang, W., Lapidus, I., White, N.E., and Titarchuk, L. 1996, ApJ, 469, L17

Zhang, W. et al. 1998a, ApJ, 495, L9

Zhang, W. et al. 1998b, ApJ, 500, L171

Table 1: Parameters of the spectra $N_1(E)$ and $N_2(E)$ (3-20 keV)

Spectrum	Model	$T_1^{(1)}, T_{MCD}^{(2)}$ (keV)	$R_1^{(3)}, N_{MCD}^{(4)}$	$T_2^{(1)}$ (keV)	$R_2^{(3)}$	Index ⁽⁵⁾	$N_{PL}^{(6)}$	χ^2/DOF
$N_1(E)$	2BB+PL	0.26 ± 0.01	274 ± 47	1.06 ± 0.01	2.09 ± 0.05	3.11 ± 0.13	0.37 ± 0.22	102.1/45
	BB+MCD+PL	0.28 ± 0.01	$(9.0 \pm 3.8) \times 10^4$	1.06 ± 0.01	2.09 ± 0.05	3.08 ± 0.13	0.32 ± 0.20	107.3/45
$N_2(E)$	2BB+PL	0.25 ± 0.01	326 ± 155	1.02 ± 0.01	2.14 ± 0.07	2.65 ± 0.14	0.15 ± 0.15	61.9/45
	BB+MCD+PL	0.27 ± 0.02	$(1.3 \pm 0.9) \times 10^5$	1.02 ± 0.01	2.13 ± 0.07	2.65 ± 0.15	0.16 ± 0.16	62.5/45

Notes: (1) BB temperature; (2) The inner disk temperature in MCD; (3) Apparent BB radii in km, assuming the distance to the source is 2.5 kpc; (4) The normalization of disk BB in MCD: $((R_{in}/\text{km})/(\text{D}/2.5\text{kpc}))^2 \cos(\theta)$, where R_{in} is the inner disk radius, D the distance to the source, and θ the angle of the disk; (5) Photon spectral index; (6) photons $\text{cm}^{-2} \text{ keV}^{-1} \text{ s}^{-1}$ at 1 keV;

Table 2: Model Fit to the subtracted spectrum $N_1(E) - N_2(E)$ (2-10 keV)

T_1 (keV)	$R_1^{(1)}$ (km)	Flux1 ⁽²⁾	T_2 (keV)	$R_2^{(1)}$ (km)	Flux2 ⁽²⁾	χ^2/DOF
0.28 ± 0.03	42 ± 12	$(3.5 \pm 1.4) \times 10^{-2}$	1.15 ± 0.03	0.62 ± 0.04	$(1.5 \pm 0.2) \times 10^{-2}$	31.0/25

Notes: (1) Apparent BB radii in km for a distance of 2.5 kpc; (2) photons $\text{cm}^{-2} \text{ s}^{-1}$.

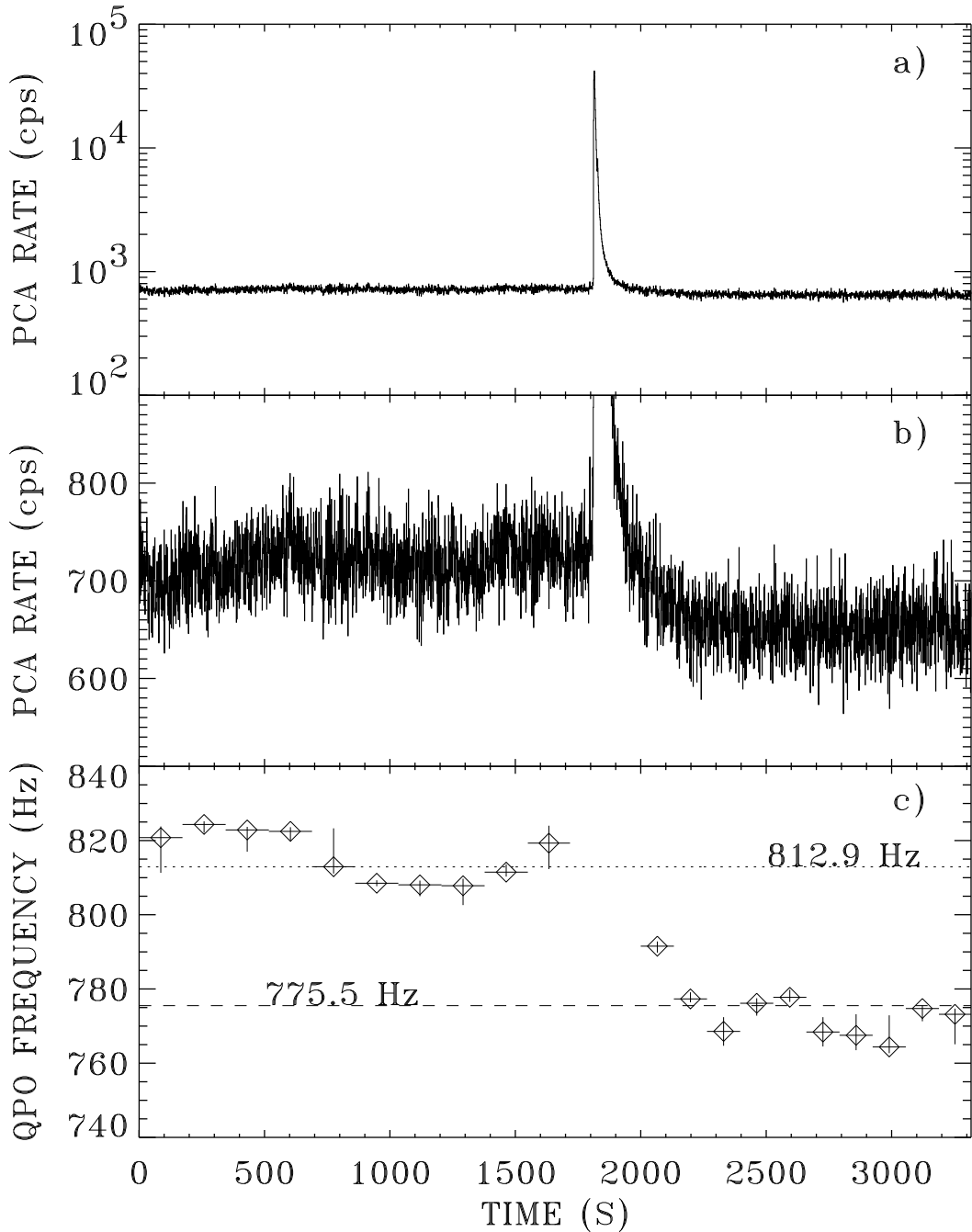


Fig. 1.— Light curve and the kilohertz QPO evolution around the X-ray burst. a) The light curve in the entire PCA energy band ($\sim 2\text{-}60$ keV) with background-subtraction. b) The flux decrease shown in detail; c) The QPO frequency evolution around the burst.

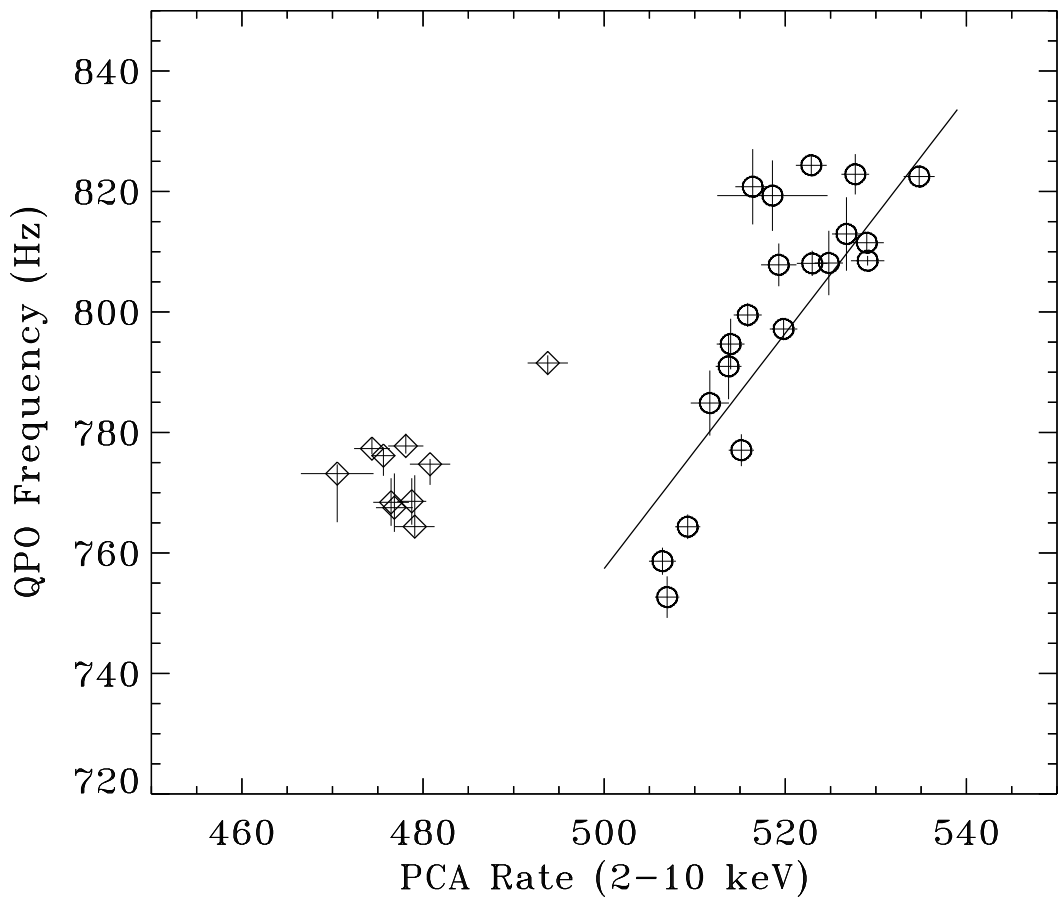


Fig. 2.— Kilohertz QPO frequency vs. PCA count rate (2-10 keV) relation observed on March 1. The data points on the left (diamonds) are taken after the X-ray burst, and those on the right (circles) are taken before the burst.

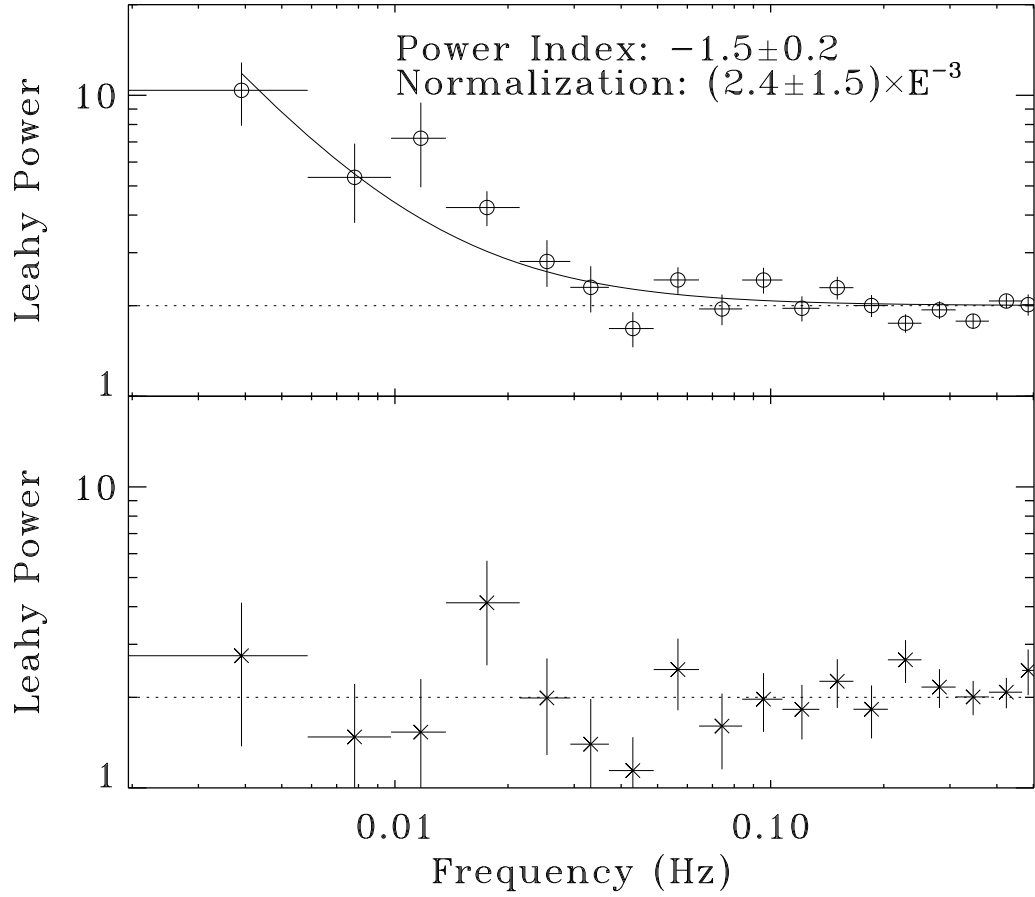


Fig. 3.— The power spectra (0.002-0.5 Hz) for the entire PCA band before and after the X-ray burst. The upper panel and the lower panel correspond to data before and after the X-ray burst, respectively. The power spectrum in the upper panel shows a VLFN component, while the power spectrum of the lower panel agrees with a white noise. The best-fit model composed of a constant white noise level of 2 and a power law VLFN is shown in the upper panel.

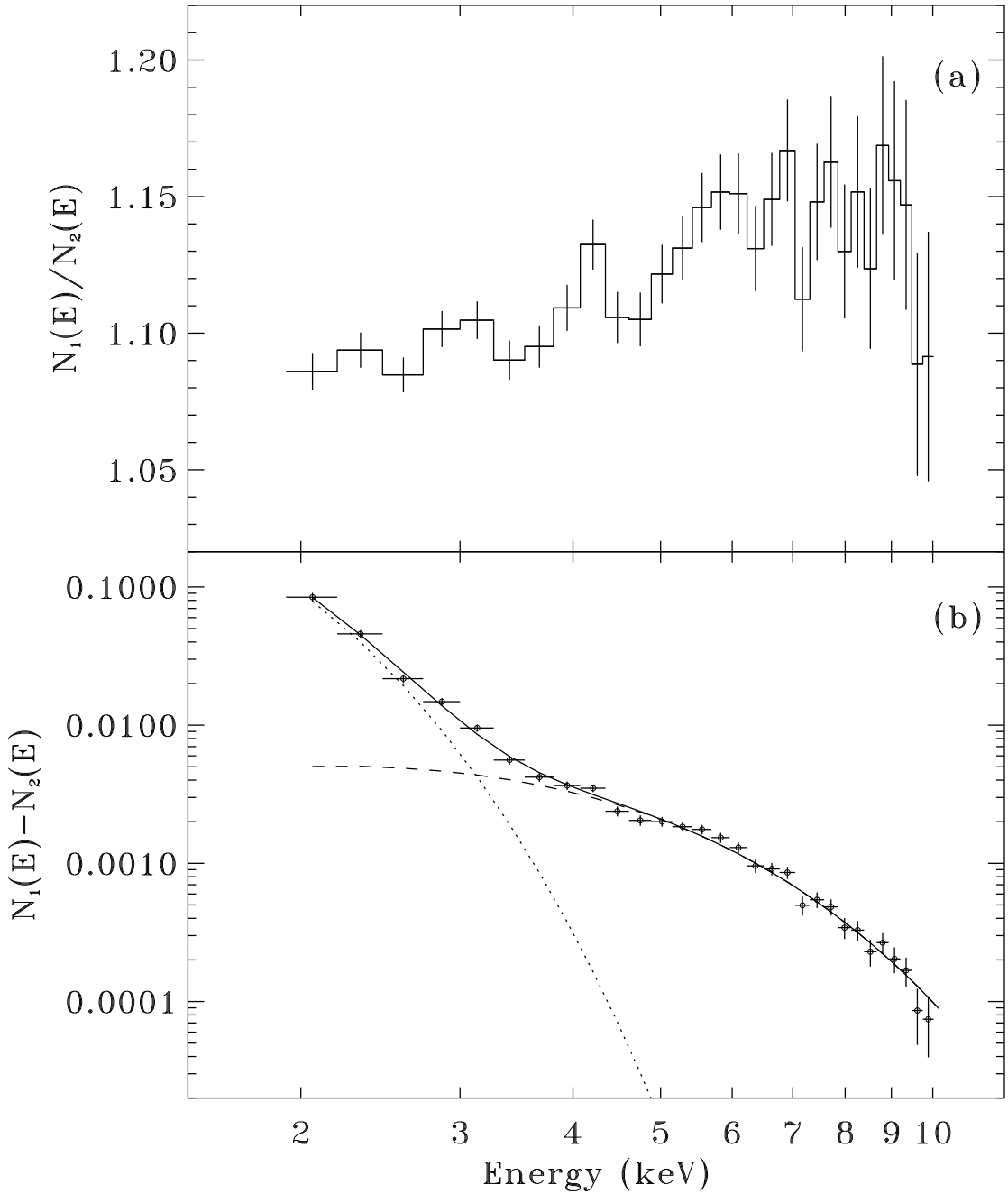


Fig. 4.— Comparison of the energy spectra before the X-ray burst, $N_1(E)$ and after the X-ray burst, $N_2(E)$ in the energy range 2-10 keV. (a) Ratio of the two spectra ($N_1(E)/N_2(E)$); (b) Difference between the two spectra ($N_1(E) - N_2(E)$) in units of photons $\text{cm}^{-2} \text{keV}^{-1} \text{s}^{-1}$ (see Table 2). The model (solid line), the 0.28 keV component (dotted line) and the 1.15 keV component (dashed line) are also shown.